IEEE Access
Multidisciplinary | Rapid Review | Open Access Journal

Received 6 October 2022, accepted 20 October 2022, date of publication 10 November 2022,
date of current version 7 December 2022.

Digital Object Identifier 10.1109/ACCESS.2022.3221411

RESEARCH ARTICLE

A Class of Explicit Divergence-Free Methods for Maxwell's Equations With Dirichlet Boundary Conditions

XIANYANG ZENG[1] AND HONGLI YANG[2]
[1]Industrial Center, Nanjing Institute of Technology, Nanjing 211167, China
[2]School of Mathematics and Physics, Nanjing Institute of Technology, Nanjing 211167, China

Corresponding author: Xianyang Zeng (zxy@njit.edu.cn)

This work was supported in part by the National Natural Science Foundation of China under Grant 11701274 and Grant 11671200, in part by the Natural Science Foundation of Jiangsu Province under Grant BK20170760, and in part by the Natural Science Foundation of Nanjing Institute of Technology under Grant CKJA202206.

ABSTRACT In this paper, we focus on the numerical solutions of Maxwell's equations with Dirichlet boundary conditions in rectangular coordinate. A class of explicit methods is derived by using an effective solver for a system of ordinary differential equations which is obtained by approximating on spatial fields. A significant advantage of this class of methods is their simplicity and their ease of implementation. The error estimates presented in this paper show that the numerical solutions obtained by this class of methods is of high-order. The main advantage of this class of methods is that it is divergence-free.

INDEX TERMS Computation theory, Dirichlet boundary value problem, divergence-free methods, electromagnetic propagation, Maxwell's equations, time-domain methods, structure-preserving algorithms.

I. INTRODUCTION

The research of electromagnetic field has affected various fields of science and technology. The computational electromagnetics provides a new and important measure for more and more complex modeling and simulations, optimization design and other problems in practical electromagnetic field engineering. There have been many methods or algorithms for solving Maxwell's equations numerically.

Recently, a great deal of attention has been paid on the direct time-domain method for numerical electromagnetics, for instance, the time-domain integral equation method [7], [9], [10], [16], [17], [22], [32], [45], the finite element time-domain method [1], [13], [14], [24], [29] and the finite difference time-domain algorithm [5], [6], [11], [12], [18], [26], [28], [29], [46]. These methods are simple and flexible, but most of them are implicit and conditionally stable. This implies that the proof of unique solvability for the underlying system of implicit equations is required, and that the computational cost is huge.

The associate editor coordinating the review of this manuscript and approving it for publication was Guido Lombardi.

Therefore, it is reasonable to design and analyse unconditionally stable and more efficient algorithms. In 2016, Wu and Liu introduced a kind of methods called as the semi-discrete method [20], [23], [34], [35], [44]. These methods can be investigated by two steps. At first a semi-discrete system of the original equations is derived via classical discrete approximations on spatial fields. Then, some special effective solvers are used for the semi-discrete system which is normally a system of ordinary differential equations. In this paper, the main aim of this paper is to propose a class of explicit semi-discrete methods for Maxwell's equations with Dirichlet boundary conditions via the rectangular coordinate analysis.

The outline of this paper is as follows. In Section II, we first give a short overview of the differential forms of Maxwell's equations under initial and Dirichlet boundary conditions. In Section III, we present the class of explicit semi-discrete methods. And in Section IV some numerical experiments are implemented. The last section is conclusions.

II. MAXWELL's EQUATIONS

In this paper, we are interested in Maxwell's equations without a source field in linear, homogeneous, isotropic and

lossless medium which are expressed in the coupled form (see, e.g. [30], [31], [32]):

$$\nabla \times \boldsymbol{\mathcal{E}}(x, y, z, t) = -\mu \frac{\partial \boldsymbol{\mathcal{H}}}{\partial t}(x, y, z, t), \tag{1}$$

$$\nabla \times \boldsymbol{\mathcal{H}}(x, y, z, t) = \varepsilon \frac{\partial \boldsymbol{\mathcal{E}}}{\partial t}(x, y, z, t), \tag{2}$$

$$\nabla \cdot \boldsymbol{\mathcal{E}}(x, y, z, t) = 0, \tag{3}$$

and

$$\nabla \cdot \boldsymbol{\mathcal{H}}(x, y, z, t) = 0, \tag{4}$$

where $\mu > 0, \varepsilon > 0$, and $\boldsymbol{\mathcal{E}}(x, y, z, t)$ and $\boldsymbol{\mathcal{H}}(x, y, z, t)$ are the electric and the magnetic fields with the initial conditions

$$\boldsymbol{\mathcal{E}}^{(0)} = \boldsymbol{\mathcal{E}}(x, y, z, t_0), \quad \boldsymbol{\mathcal{H}}^{(0)} = \boldsymbol{\mathcal{H}}(x, y, z, t_0), \tag{5}$$

on cubic domain $\Omega = [-1, 1]^3$, and the Dirichlet boundary conditions are given

$$\boldsymbol{\mathcal{E}}|_\Gamma = \boldsymbol{\mathcal{E}}(x, y, z, t)|_\Gamma, \quad \boldsymbol{\mathcal{H}}|_\Gamma = \boldsymbol{\mathcal{H}}(x, y, z, t)|_\Gamma, \tag{6}$$

on $\Gamma = \partial\Omega \times [t_0, T]$. These expressions are valid under the condition that the field vectors are single-valued, bounded, continuous functions of position and time, and exhibit continuous derivatives.

To uncouple these equations, using the well-known potential theory in electromagnetics [2], [29], we can conveniently obtain

$$\frac{\partial^2}{\partial t^2}\boldsymbol{\mathcal{H}}(x, y, z, t) - \frac{1}{\mu\varepsilon}\nabla^2 \boldsymbol{\mathcal{H}}(x, y, z, t) = \mathbf{0}, \tag{7}$$

where $\frac{\partial}{\partial t}\boldsymbol{\mathcal{H}}(x, y, z, t) = -\frac{1}{\mu}\nabla \times \boldsymbol{\mathcal{E}}(x, y, z, t)$, and

$$\frac{\partial^2}{\partial t^2}\boldsymbol{\mathcal{E}}(x, y, z, t) - \frac{1}{\mu\varepsilon}\nabla^2 \boldsymbol{\mathcal{E}}(x, y, z, t) = \mathbf{0}, \tag{8}$$

where $\frac{\partial}{\partial t}\boldsymbol{\mathcal{E}}(x, y, z, t) = \frac{1}{\varepsilon}\nabla \times \boldsymbol{\mathcal{H}}(x, y, z, t)$, on noticing the fact that $\nabla^2 = \nabla(\nabla\cdot) - \nabla \times (\nabla\times)$.

III. CONSERVATIVE METHODS

A. APPROXIMATIONS OF DIFFERENTIAL OPERATORS IN PHYSICAL SPACE

This subsection is devoted to the differentiation matrices which approximate the second-order partial differential operator in physical space. Since it is a nonperiodic problem on $[-1, 1]$, we consider the Gauss-Lobatto points

$$x_i = \cos\frac{\pi i}{N}, \quad i = 0, 1, 2, \ldots, N. \tag{9}$$

Because of round-off erros, (see [25]) identified by Baylies et al. (1994), the off-diagonal entries $d_{i,j}^{[2]}$, $j \neq i$ of the second-order differentiation matrix $D^{[2]} = \left(d_{i,j}^{[2]}\right)_{N\times N}$ is calculated by

$$d_{i,j}^{[2]} = \frac{(-1)^{i+j}}{\bar{c}_j}\frac{x_i^2 + x_i x_j - 2}{(1 - x_i^2)(x_i - x_j)^2}, \tag{10}$$

if $1 \le i \le N-1,\ 0 \le j \le N,\ i \neq j$;

$$d_{0,j}^{[2]} = \frac{2}{3}\frac{(-1)^j}{\bar{c}_j}\frac{(2N^2+1)(1-x_j) - 6}{(1-x_j)^2}, \tag{11}$$

if $1 \le j \le N$;

$$d_{N,j}^{[2]} = \frac{2}{3}\frac{(-1)^{j+N}}{\bar{c}_j}\frac{(2N^2+1)(1+x_j) - 6}{(1+x_j)^2}, \tag{12}$$

if $0 \le j \le N-1$; and the diagonal entries $d_{i,i}^{[2]}$ by

$$d_{i,i}^{[2]} = -\sum_{j=0,\, j\neq i}^{N} d_{i,j}^{[2]}, \quad i = 0, 1, \ldots, N, \tag{13}$$

where $\bar{c}_0 = \bar{c}_N = 2$ and $\bar{c}_j = 1$ for $1 \le j \le N-1$.

B. APPROXIMATION OF A DIFFERENTIAL EQUATION IN SCALAR CASE

In this subsection, we consider the linear wave equation [27], [34]:

$$\frac{\partial^2}{\partial t^2}u - \frac{1}{\mu\varepsilon}\left(\frac{\partial^2}{\partial x^2}u + \frac{\partial^2}{\partial y^2}u + \frac{\partial^2}{\partial z^2}u\right) = 0, \tag{14}$$

for the scalar function $u = u(x, y, z, t)$, where $(x, y, z) \in \Omega = [-1, 1]^3$, $t \in [t_0, T]$, with the initial conditions and the Dirichlet boundary conditions are given by

$$u_0(x, y, z) = u(x, y, z, t_0),\ u(x, y, z, t)|_\Gamma = g(x, y, z, t),$$

for $(x, y, z) \in \Omega$, $t \in [t_0, T]$, where $\Gamma = \partial\Omega$. Equation (14) is spatially discretised by the collocation method based on the Gauss-Lobatto points

$$x_i = \cos\frac{\pi i}{N_x}, \quad i = 0, 1, 2, \ldots, N_x,$$

$$y_j = \cos\frac{\pi j}{N_y}, \quad j = 0, 1, 2, \ldots, N_y,$$

$$z_k = \cos\frac{\pi k}{N_z}, \quad k = 0, 1, 2, \ldots, N_z,$$

where the spatial grid numbers N_x, N_y and N_z are integers. We here denote the second differentiation matrices in the x-, y-, and z-directions, respectively, by

$$D^{X,[2]} = \left(d_{i,r}^{X,[2]}\right)_{N_x\times N_x}, \quad i, r = 0, 1, 2, \ldots, N_x$$

$$D^{Y,[2]} = \left(d_{j,r}^{Y,[2]}\right)_{N_y\times N_y}, \quad j, r = 0, 1, 2, \ldots, N_y$$

$$D^{Z,[2]} = \left(d_{k,r}^{Z,[2]}\right)_{N_z\times N_z}, \quad k, r = 0, 1, 2, \ldots, N_z,$$

analogous to the matrix $D^{[2]}$ defined in the one dimensional case. In this paper, without loss generality we consider the domain with spatial grid numbers $N_x = N_y = N_z = 18$. Using MATLAB software, we can check these three differentiation matrices are all negative definite since each eigenvalue

of these matrices is negative, with the given spatial grid numbers.

By setting to zero the residual at the inner collocation points, we obtain the collocation equations

$$\frac{d^2}{dt^2}u(x_i,y_j,z_k,t)-\frac{1}{\mu\varepsilon}\left[\sum_{r=0}^{N_x}d_{i,r}^{X,[2]}u(x_r,y_j,z_k,t)+\sum_{r=0}^{N_y}d_{j,r}^{Y,[2]}u(x_i,y_r,z_k,t)+\sum_{r=0}^{N_z}d_{k,r}^{Z,[2]}u(x_i,y_j,z_r,t)\right]=0, \tag{15}$$

for $i=1,2,\ldots,N_x-1$, $j=1,2,\ldots,N_y-1$, and $k=1,2,\ldots,N_z-1$, where the inner collocation points form an open discretised domain, denoted by Ω_N, i.e.,

$$\Omega_N=\Big\{(x_i,y_j,z_k):\quad i=1,2,\ldots,N_x-1;\ j=1,2,\ldots,N_y-1;\ k=1,2,\ldots,N_z-1\Big\}.$$

From the boundary conditions, we have the boundary values expressed by

$$\begin{aligned}u(x_0,y_j,z_k,t)&=g(1,y_j,z_k,t),\\ u(x_{N_x},y_j,z_k,t)&=g(-1,y_j,z_k,t),\\ u(x_i,y_0,z_k,t)&=g(x_i,1,z_k,t),\\ u(x_i,y_{N_y},z_k,t)&=g(x_i,-1,z_k,t),\\ u(x_i,y_j,z_0,t)&=g(x_i,y_j,1,t),\\ u(x_i,y_j,z_{N_z},t)&=g(x_i,y_j,-1,t).\end{aligned} \tag{16}$$

By inserting (16) into (15), we have

$$\frac{d^2}{dt^2}u_{i,j,k}(t)-\frac{1}{\mu\varepsilon}\left[\sum_{r=1}^{\overline{N}_x}d_{i,r}^{X,[2]}u_{i,j,k}(t)+\sum_{r=1}^{\overline{N}_y}d_{j,r}^{Y,[2]}u_{i,j,k}(t)+\sum_{r=1}^{\overline{N}_z}d_{k,r}^{Z,[2]}u_{i,j,k}(t)\right]=\frac{1}{\mu\varepsilon}\bar{g}_{i,j,k}(t), \tag{17}$$

where $\overline{N}_x=N_x-1$, $\overline{N}_y=N_y-1$, and $\overline{N}_z=N_z-1$, $u_{i,j,k}(t)=u(x_i,y_j,z_k,t)$ and

$$\begin{aligned}\bar{g}_{i,j,k}(t)=&\,d_{i,0}^{X,[2]}g(1,y_j,z_k,t)+d_{i,N_x}^{X,[2]}g(-1,y_j,z_k,t)\\ &+d_{j,0}^{Y,[2]}g(x_i,1,z_k,t)+d_{j,N_y}^{Y,[2]}g(x_i,-1,z_k,t)\\ &+d_{k,0}^{Z,[2]}g(x_i,y_j,1,t)+d_{k,N_z}^{Z,[2]}g(x_i,y_j,-1,t).\end{aligned}$$

This system of ordinary differential equations can be written in matrix form,

$$\frac{d^2}{dt^2}U(t)-\frac{1}{\mu\varepsilon}AU(t)=G(t), \tag{18}$$

with the initial conditions

$$U(t_0)=U_0, \tag{19}$$

at every spacial collocation point (x_i,y_j,z_k) in the open discretised domain Ω_N, where we denote by $U(t)$ the semidiscretised solution which approximates the exact function $u(x,y,z,t)$ in the open discretised domain Ω_N. The unknown $\overline{N}_x\overline{N}_y\overline{N}_z$-dimensional column vector $U(t)$ is ordered by row and horizontal section (the boundary conditions have been incorporated into $U(t)$). More precisely, we introduce the $\overline{N}_x$-dimensional vector $U_{j,k}(t)$:

$$U_{j,k}(t)=\Big(u(x_1,y_j,z_k,t),\ldots,u(x_{\overline{N}_x},y_j,z_k,t)\Big)^{\mathsf{T}},$$

for $j=1,\ldots,\overline{N}_y$, $k=1,\ldots,\overline{N}_z$. We then define the $\overline{N}_x\overline{N}_y$-dimensional vector $U_k(t)$ by

$$U_k(t)=\Big(U_{1,k}(t),\ldots,U_{\overline{N}_y,k}(t)\Big)^{\mathsf{T}},$$

for $k=1,\ldots,\overline{N}_z$, and, finally, $U(t)$ is the $\overline{N}_x\overline{N}_y\overline{N}_z$-dimensional vector defined by

$$U(t)=\Big(U_1(t),\ldots,U_{\overline{N}_z}(t)\Big)^{\mathsf{T}}.$$

A is $(\overline{N}_x\overline{N}_y\overline{N}_z)\times(\overline{N}_x\overline{N}_y\overline{N}_z)$ differentiation matrix, and can be written in terms of the tensor product form

$$A=\mathcal{I}_z\otimes\mathcal{I}_y\otimes\mathcal{D}_{xx}+\mathcal{I}_z\otimes\mathcal{D}_{yy}\otimes\mathcal{I}_x+\mathcal{D}_{zz}\otimes\mathcal{I}_y\otimes\mathcal{I}_x, \tag{20}$$

where the differentiation matrices $\mathcal{D}_{xx}$, $\mathcal{D}_{yy}$, and $\mathcal{D}_{zz}$ are of dimensions $\overline{N}_x\times\overline{N}_x$, $\overline{N}_y\times\overline{N}_y$, and $\overline{N}_z\times\overline{N}_z$, respectively, yielded from the discretisations of the second-order partial differential operators ∂_{xx}, ∂_{yy}, and ∂_{zz}. Taking $\mathcal{D}_{xx}$ as example, $\mathcal{D}_{xx}=\left(d_{i,r}^{X}\right)$, $i,r=1,2,\ldots,\overline{N}_x$ is defined by $d_{i,r}^{X}=d_{i,r}^{X,[2]}$. And the identity matrices $\mathcal{I}_x$, $\mathcal{I}_y$, and $\mathcal{I}_z$ in the x-, y-, and z-directions have the same dimensions as $\mathcal{D}_{xx}$, $\mathcal{D}_{yy}$, and $\mathcal{D}_{zz}$, respectively. Lastly, the right-hand side $\overline{N}_x\overline{N}_y\overline{N}_z$-dimensional vector $G(t)$ in Eq. (18) is constructed in the same way as $U(t)$, and with components $g_{i,j,k}(t)=\frac{1}{\mu\varepsilon}\bar{g}_{i,j,k}(t)$. From the property of Kronecker product, we have that the matrix A is negative definite.

C. THE NUMERICAL METHODS

For Maxwell's equations, we have the following ordinary differential equations

$$\begin{aligned}\frac{d^2}{dt^2}E_w(t)+LE_w(t)&=P_w(t),\\ \frac{d^2}{dt^2}H_w(t)+LH_w(t)&=Q_w(t),\end{aligned} \tag{21}$$

where the unknowns $E_w(t)$, and $H_w(t)$ are the column vectors which approximate functions $\mathcal{E}_w(x,y,z,t)$, and $\mathcal{H}_w(x,y,z,t)$, respectively, for $w=x$, y, or z. Precisely speaking, taking $E_x(t)\in\mathbb{R}^{\overline{N}_x\overline{N}_y\overline{N}_z\times1}$ as examples, we have

$$E_x(t)=\left(\Big(E_x(t)\Big)_{i,j,k}\right)=\begin{pmatrix}\mathcal{E}_x(x_1,y_1,z_1,t)\\ \vdots\\ \mathcal{E}_x(x_{\overline{N}_x},y_{\overline{N}_y},z_{\overline{N}_z},t)\end{pmatrix}.$$

In Eq. (21), $P_w(t)$ and $Q_w(t)$ are functions calculated from the boundary conditions, analogous to the vector $G(t)$ in (18)

in the scalar case, and $L = -\frac{1}{\mu\varepsilon}A$ where A is an $(\overline{N}_x\overline{N}_y\overline{N}_z) \times (\overline{N}_x\overline{N}_y\overline{N}_z)$ matrix given by (20). So the matrix L is positive definite, which coincide with the positive (semi)definite of the operator $-\frac{1}{\mu\varepsilon}\nabla^2$ (see. e.g. [15], [19], [21], [34], [35], [36], [37], [38]), in the sense of structure preservation. And we then can introduce two convergent matrix-valued functions $\phi_i\big(h_t^2L\big)$ for $i = 0, 1$, which are defined by

$$\phi_i\big(h_t^2L\big) = \sum_{k=0}^{\infty} \frac{(-1)^k}{(2k+i)!} h_t^{2k} L^k, \quad i = 0, 1. \tag{22}$$

We have that these two matrix-valued functions $\phi_i(\cdot)$ are bounded, for $i = 0, 1$. With respect to the matrix-valued functions $\phi_i(\cdot)$ for $i = 0, 1, \ldots$, the reader is referred to [33], [36], [39], [40], [41], [42], [43], [44], [47], [48] for details. From the matrix-variation-of-constants formula [42], the exact solutions of Eq. (21) and their derivatives satisfy

$$\begin{aligned} E_w(t) &= \phi_0\big(\hat{L}\big)E_w(t_0) + h_t\phi_1\big(\hat{L}\big)\tfrac{d}{dt}E_w(t_0) \\ &\quad + h_t^2\int_0^1 (1-\xi)\phi_1\big((1-\xi)^2\hat{L}\big)P_w(t_0+h_t\xi)d\xi, \end{aligned} \tag{23}$$

$$\begin{aligned} \tfrac{d}{dt}E_w(t) &= -h_t\phi_1\big(\hat{L}\big)LE_w(t_0) + \phi_0\big(\hat{L}\big)\tfrac{d}{dt}E_w(t_0) \\ &\quad + h_t\int_0^1 \phi_0((1-\xi)^2\hat{L})P_w\big(t_0+h_t\xi\big)d\xi, \end{aligned} \tag{24}$$

$$\begin{aligned} H_w(t) &= \phi_0\big(\hat{L}\big)H_w(t_0) + h_t\phi_1\big(\hat{L}\big)\tfrac{d}{dt}H_w(t_0) \\ &\quad + h_t^2\int_0^1 (1-\xi)\phi_1\big((1-\xi)^2\hat{L}\big)Q_w(t_0+h_t\xi)d\xi, \end{aligned} \tag{25}$$

and

$$\begin{aligned} \tfrac{d}{dt}H_w(t) &= -h_t\phi_1\big(\hat{L}\big)LH_w(t_0) + \phi_0\big(\hat{L}\big)\tfrac{d}{dt}H_w(t_0) \\ &\quad + h_t\int_0^1 \phi_0((1-\xi)^2\hat{L})Q_w\big(t_0+h_t\xi\big)d\xi, \end{aligned} \tag{26}$$

where $t = t_0 + h_t$, $\hat{L} = h_t^2L$. Now we discrete the first order partial derivatives of electric field and magnetic field with respect to time, i.e. (1) and (2), we have

$$\begin{aligned} \tfrac{d}{dt}E_w(t) &= \frac{1}{\varepsilon}\widetilde{H}_w(t), \\ \tfrac{d}{dt}H_w(t) &= -\frac{1}{\mu}\widetilde{E}_w(t), \end{aligned} \tag{27}$$

where $\widetilde{E}_x(t)$, $\widetilde{E}_y(t)$, $\widetilde{E}_z(t)$, $\widetilde{H}_x(t)$, $\widetilde{H}_y(t)$, and $\widetilde{H}_z(t)$ are the approximates of the first, second, and third entry of the curls $\nabla \times \boldsymbol{\mathcal{E}}$ and $\nabla \times \boldsymbol{\mathcal{H}}$, respectively, at all inner spacial collocation points (x_i, y_j, z_k) in the open discretised domain Ω_N. Precisely speaking, taking $\widetilde{E}_x(t) \in \mathbb{R}^{\overline{N}_x\overline{N}_y\overline{N}_z\times 1}$ as examples, its entry satisfies $\big(\widetilde{E}_x(t)\big)_{i,j,k} = \big(\nabla \times \boldsymbol{\mathcal{E}}\big)_x(x_i, y_j, z_k, t)$. In this discretisation of the curls, we here remark that $\widetilde{E}_w(t)$ (for $w = x$, y or z) are all regarded as unknown, instead of making a discretisation for the $\nabla\times$ operator.

Now, we design two efficient schemes, by making time-discretisation and taking the truncations of functions $\phi_0\big(c^2h_t^2L\big)$ and $\phi_1\big(c^2h_t^2L\big)$ with p terms, (denoted as $\Phi_0(p, c)$ and $\Phi_1(p, c)$) respectively, i.e.,

$$\begin{cases} \Phi_0(p,c) \triangleq I - \frac{1}{2!}c^2h_t^2L + \frac{1}{4!}c^4h_t^4L^2 + \cdots \\ \qquad\qquad +(-1)^p\frac{1}{(2p)!}c^{2p}h_t^{2p}L^p, \\ \Phi_1(p,c) \triangleq I - \frac{1}{3!}c^2h_t^2L + \frac{1}{5!}c^4h_t^4L^2 + \cdots \\ \qquad\qquad +(-1)^p\frac{1}{(2p+1)!}c^{2p}h_t^{2p}L^p. \end{cases} \tag{28}$$

Thus, we obtain the scheme to have the numerical solutions $\big(E_w^{(n+1)}, \widetilde{H}_w^{(n+1)}\big)$ as follows:

$$\begin{cases} E_w^{(n+1)} = \Phi_0E_w^{(n)} + \frac{1}{\varepsilon}h_t\Phi_1\widetilde{H}_w^{(n)} \\ \qquad\qquad +h_t^2\sum_{i=1}^{s} b_i(1-c_i)\Psi_{1,i}P_w(t_n+c_ih_t), \\ \widetilde{H}_w^{(n+1)} = -\varepsilon h_t\Phi_1LE_w^{(n)} + \Phi_0\widetilde{H}_w^{(n)} \\ \qquad\qquad +\varepsilon h_t\sum_{i=1}^{s} b_i\Psi_{0,i}P_w(t_n+c_ih_t), \end{cases} \tag{29}$$

where $\Phi_0 := \Phi_0(p, 1)$, $\Phi_1 := \Phi_1(p, 1)$, $\Psi_{0,i} := \Phi_0(p-1, 1-c_i)$, and $\Psi_{1,i} := \Phi_1(p-1, 1-c_i)$. The scheme to have $\big(H_w^{(n+1)}, \widetilde{E}_w^{(n+1)}\big)$ can be derived as follows:

$$\begin{cases} H_w^{(n+1)} = \Phi_0H_w^{(n)} - \frac{1}{\mu}h_t\Phi_1\widetilde{E}_w^{(n)} \\ \qquad\qquad +h_t^2\sum_{i=1}^{s} b_i(1-c_i)\Psi_{1,i}Q_w(t_n+c_ih_t), \\ \widetilde{E}_w^{(n+1)} = \mu h_t\Phi_1LH_w^{(n)} + \Phi_0\widetilde{E}_w^{(n)} \\ \qquad\qquad -\mu h_t\sum_{i=1}^{s} b_i\Psi_{0,i}Q_w(t_n+c_ih_t). \end{cases} \tag{30}$$

In the above two schemes (29) and (30), the notations $E_w^{(n)}$, $H_w^{(n)}$, $\widetilde{E}_w^{(n)}$, and $\widetilde{H}_w^{(n)}$ approximate $E_w(t)$, $H_w(t)$, $\widetilde{E}_w(t)$, and $\widetilde{H}_w(t)$ at $t_n = t_0 + nh_t$, respectively, for $w = x$, y, or z. And in these two schemes, the nodes c_i and coefficients b_i, for $i = 1, \ldots, s$, of numerical integration formula are chosen to make the scheme have a high time accuracy.

Since the formula (23)–(26) are exactly true for the partial derivative of exact solutions, with respect to the spatial variable, the arguments developed for the vectors $E_w^{(n)}$, $\widetilde{H}_w^{(n)}$, $H_w^{(n)}$, and $\widetilde{E}_w^{(n)}$ also apply to $\big(E^v\big)_w^{(n)}$, $\big(\widetilde{H}^v\big)_w^{(n)}$, $\big(H^v\big)_w^{(n)}$, and $\big(\widetilde{E}^v\big)_w^{(n)}$ for $w = x, y, z$, where the entries of these four vectors are

$$\begin{aligned} \Big(\big(E^v\big)_w\Big)_{i,j,k}^{(n)} &\approx \frac{\partial}{\partial v}\boldsymbol{\mathcal{E}}_w(x_i, y_j, z_k, t_n), \\ \Big(\big(\widetilde{H}^v\big)_w\Big)_{i,j,k}^{(n)} &\approx \frac{\partial}{\partial v}\big(\nabla \times \boldsymbol{\mathcal{H}}\big)_w(x_i, y_j, z_k, t_n), \end{aligned}$$

and

$$\left(\left(H^{v}\right)_{w}\right)_{i,j,k}^{(n)} \approx \frac{\partial}{\partial v}\mathcal{H}_{w}(x_i, y_j, z_k, t_n),$$
$$\left(\left(\widetilde{E}^{v}\right)_{w}\right)_{i,j,k}^{(n)} \approx \frac{\partial}{\partial v}\left(\nabla \times \boldsymbol{\mathcal{E}}\right)_{w}(x_i, y_j, z_k, t_n).$$

Precisely, the vectors $\left(E^{v}\right)_{w}^{(n)}$ and the coupled $\left(\widetilde{H}^{v}\right)_{w}^{(n)}$ can be calculated by

$$\begin{cases} \left(E^{v}\right)_{w}^{(n+1)} = \Phi_0\left(E^{v}\right)_{w}^{(n)} + \frac{1}{\varepsilon}h_t\Phi_1\left(\widetilde{H}^{v}\right)_{w}^{(n)} \\ \qquad\qquad +h_t^2\sum_{i=1}^{s} b_i(1-c_i)\Psi_{1,i}P_{w}^{v}(t_n + c_i h_t), \\ \left(\widetilde{H}^{v}\right)_{w}^{(n+1)} = -\varepsilon h_t\Phi_1 L\left(E^{v}\right)_{w}^{(n)} + \Phi_0\left(\widetilde{H}^{v}\right)_{w}^{(n)} \\ \qquad\qquad +\varepsilon h_t\sum_{i=1}^{s} b_i\Psi_{0,i}P_{w}^{v}(t_n + c_i h_t), \end{cases} \tag{31}$$

and the vectors $\left(H^{v}\right)_{w}^{(n)}$ and the coupled $\left(\widetilde{E}^{v}\right)_{w}^{(n)}$ can be yielded from

$$\begin{cases} \left(H^{v}\right)_{w}^{(n+1)} = \Phi_0\left(H^{v}\right)_{w}^{(n)} - \frac{1}{\mu}h_t\Phi_1\left(\widetilde{E}^{v}\right)_{w}^{(n)} \\ \qquad\qquad +h_t^2\sum_{i=1}^{s} b_i(1-c_i)\Psi_{1,i}Q_{w}^{v}(t_n + c_i h_t), \\ \left(\widetilde{E}^{v}\right)_{w}^{(n+1)} = \mu h_t\Phi_1 L\left(H^{v}\right)_{w}^{(n)} + \Phi_0\left(\widetilde{E}^{v}\right)_{w}^{(n)} \\ \qquad\qquad -\mu h_t\sum_{i=1}^{s} b_i\Psi_{0,i}Q_{w}^{v}(t_n + c_i h_t), \end{cases} \tag{32}$$

where $P_{w}^{v}(t)$ and $Q_{w}^{v}(t)$ are functions calculated from the boundary conditions, analogous to that in (18) in the scalar case, the initial values are known exactly, since $\mathcal{E}_w(x, y, z, t_0)$ and $\mathcal{H}_w(x, y, z, t_0)$ are entries of the initial conditions of the underlying Maxwell's equations for v, $w = x, y,$ or z.

Under these notations described above, we can monitor much numerical behaviour, for instance, the numerical changes in the divergences. In this paper, we define the *numerical electric divergence* and the *numerical magnetic divergence* as

$$\left(E^{x}\right)_{x}^{(n)} + \left(E^{y}\right)_{y}^{(n)} + \left(E^{z}\right)_{z}^{(n)}, \tag{33}$$

and

$$\left(H^{x}\right)_{x}^{(n)} + \left(H^{y}\right)_{y}^{(n)} + \left(H^{z}\right)_{z}^{(n)}, \tag{34}$$

and denoted as DIV_E and DIV_H, respectively.

The divergence-free analysis of magnetic is an important aspect of numerical methods for Maxwells equations. Accordingly, in the process of numerical simulation, the magnetic divergences would be forced to be corrected to zeros at any space collocation points, by an additional procedure [3], [4], [8], [30]. The first divergence correction method was proposed by Smith [30] in 1996. In this paper, we will show that the numerical solutions of our schemes are magnetic divergence-free naturally.

Before ending this section, we here remark that the numerical methods obtained from these four schemes (29), (30), (31) and (32) are uncoupled, one-step and explicit. Moreover the methods can be implement with low computational cost and memory storage, since they all split one big recurrence into six small ones. The dimensions of the matrices L, Φ_0, Φ_1, $\Psi_{0,i}$, and $\Psi_{1,i}$ are all $(\overline{N}_x\overline{N}_y\overline{N}_z) \times (\overline{N}_x\overline{N}_y\overline{N}_z)$ which is much lower than $(6\overline{N}_x\overline{N}_y\overline{N}_z) \times (6\overline{N}_x\overline{N}_y\overline{N}_z)$ as the traditional methods. And fortunately, the calculations is really cheap, since the values of p and the stage number s can be both small.

IV. NUMERICAL EXPERIMENTS

This section describes some numerical results of applying our method to the travelling wave solutions and the standing wave solutions of Maxwell's equations.

Example 1: We consider Maxwell's equations having travelling wave solution [17] ($\varepsilon = \mu = 1$)

$$\begin{aligned} &\mathcal{E}_x = \mathcal{E}_x, \mathcal{H}_x = \sqrt{3}\mathcal{E}_x, \\ &\mathcal{E}_y = -2\mathcal{E}_x, \mathcal{H}_y = 0, \\ &\mathcal{E}_z = \mathcal{E}_x, \mathcal{H}_z = -\sqrt{3}\mathcal{E}_x, \end{aligned} \tag{35}$$

where $\mathcal{E}_x = \cos(2\pi(x + y + z) - 2\sqrt{3}\pi t)$.

We consider the Dirichlet boundary conditions and take the analytical solutions (35) at $t_0 = 0$ on the cube $[-1, 1]^3$ as the initial conditions. Namely, we have the numerical electric field vector at initial time in the x-direction $E_x^{(0)}$ and the corresponding numerical curl of magnetic field vector in the x-direction $\widetilde{H}_x^{(0)}$, with the entries

$$\begin{cases} \left(E_x\right)_{i,j,k}^{(0)} = \cos(2\pi(x_i + y_j + z_k)), \\ \left(\widetilde{H}_x\right)_{i,j,k}^{(0)} = 2\sqrt{3}\pi\,\sin(2\pi(x_i + y_j + z_k)), \end{cases} \tag{36}$$

for $i = 1, 2, \ldots, \overline{N}_x$, $j = 1, 2, \ldots, \overline{N}_y$, $k = 1, 2, \ldots, \overline{N}_z$. Then we have H_x and $\widetilde{E}_x$ as follows:

$$\begin{cases} H_x^{(0)} = \sqrt{3}E_x^{(0)}, \\ \widetilde{E}_x^{(0)} = -\sqrt{3}\widetilde{H}_x^{(0)}. \end{cases} \tag{37}$$

From the proportional among different fields, we have the numerical solutions in y-direction

$$\begin{cases} E_y^{(0)} = -2E_x^{(0)}, \\ \widetilde{H}_y^{(0)} = -2\widetilde{H}_x^{(0)}, \end{cases} \quad \begin{cases} H_y^{(0)} = \mathbf{0}, \\ \widetilde{E}_y^{(0)} = \mathbf{0}, \end{cases} \tag{38}$$

and the numerical solutions in z-direction

$$\begin{cases} E_z^{(0)} = E_x^{(0)}, \\ \widetilde{H}_z^{(0)} = \widetilde{H}_x^{(0)}, \end{cases} \quad \begin{cases} H_z^{(0)} = -H_x^{(0)}, \\ \widetilde{E}_z^{(0)} = -\widetilde{E}_x^{(0)}. \end{cases} \tag{39}$$

In the schemes (29)–(30), the entries of the vector $P_x(t)$ are

$$\begin{aligned} \left(P_x(t)\right)_{i,j,k} = \frac{1}{\mu\varepsilon}\Big(&d_{i,0}^{[2]}\cos(2\pi(1 + y_j + z_k) - 2\sqrt{3}\pi t) \\ &+d_{i,N_x}^{[2]}\cos(2\pi(-1 + y_j + z_k) - 2\sqrt{3}\pi t) \\ &+d_{j,0}^{[2]}\cos(2\pi(x_i + 1 + z_k) - 2\sqrt{3}\pi t) \\ &+d_{j,N_y}^{[2]}\cos(2\pi(x_i - 1 + z_k) - 2\sqrt{3}\pi t) \\ &+d_{k,0}^{[2]}\cos(2\pi(x_i + y_j + 1) - 2\sqrt{3}\pi t) \\ &+d_{k,N_z}^{[2]}\cos(2\pi(x_i + y_j - 1) - 2\sqrt{3}\pi t)\Big), \end{aligned}$$

for $i = 1, 2, \ldots, \overline{N}_x$, $j = 1, 2, \ldots, \overline{N}_y$, $k = 1, 2, \ldots, \overline{N}_z$, where $d_{r,s}^{[2]}$ are given in (10) to (13). And

$$P_y(t) = -2P_x(t),\ P_z(t) = P_x(t),$$
$$Q_x(t) = \sqrt{3}P_x(t),\ Q_y(t) = \mathbf{0},\ Q_z(t) = -\sqrt{3}P_x(t).$$

From the schemes (29) – (30), we can have the numerical electromagnetic field and then the maximum error norm, to show the approximate accuracy, which is defined by

$$L_\infty = \max\left\{\varepsilon \max_{i,j,k}\left|\boldsymbol{\mathcal{E}}(:,T) - E^{(N_t)}\right|, \mu \max_{i,j,k}\left|\boldsymbol{\mathcal{H}}(:,T) - H^{(N_t)}\right|\right\} \quad (40)$$

To investigate the numerical divergences, the corresponding initial values of the schemes (31) – (32) can be calculated exactly from the initial conditions (36), (37), (38), and (39). Precisely the entries of the vectors $\left(E^x\right)_x^{(0)}$ and $\left(\widetilde{H}^x\right)_x^{(0)}$ are as follows:

$$\begin{cases} \left(\left(E^x\right)_x\right)_{i,j,k}^{(0)} = -2\pi\,\sin(2\pi(x_i + y_j + z_k)), \\ \left(\left(\widetilde{H}^x\right)_x\right)_{i,j,k}^{(0)} = 4\sqrt{3}\pi^2\cos(2\pi(x_i + y_j + z_k)), \end{cases} \quad (41)$$

for $i = 1, 2, \ldots, \overline{N}_x, j = 1, 2, \ldots, \overline{N}_y, k = 1, 2, \ldots, \overline{N}_z$, and the vectors $\left(H^x\right)_x^{(0)}$ and $\left(\widetilde{E}^x\right)_x^{(0)}$ are

$$\begin{cases} \left(H^x\right)_x^{(0)} = \sqrt{3}\left(E^x\right)_x^{(0)} \\ \left(\widetilde{E}^x\right)_x^{(0)} = -\sqrt{3}\left(\widetilde{H}^x\right)_x^{(0)}. \end{cases} \quad (42)$$

The numerical solutions in y-direction can be expressed as follows:

$$\begin{cases} \left(E^y\right)_y^{(0)} = -2\left(E^x\right)_x^{(0)}, \\ \left(\widetilde{E}^y\right)_y^{(0)} = \mathbf{0}, \end{cases} \quad \begin{cases} \left(H^y\right)_y^{(0)} = \mathbf{0}, \\ \left(\widetilde{E}^y\right)_y^{(0)} = \mathbf{0}, \end{cases} \quad (43)$$

and the numerical solutions in z-direction expressed as follows:

$$\begin{cases} \left(E^z\right)_z^{(0)} = \left(E^x\right)_x^{(0)}, \\ \left(\widetilde{H}^z\right)_z^{(0)} = \left(\widetilde{H}^x\right)_x^{(0)}, \end{cases} \quad \begin{cases} \left(H^z\right)_z^{(0)} = -\left(H^x\right)_x^{(0)}, \\ \left(\widetilde{E}^z\right)_z^{(0)} = -\left(\widetilde{E}^x\right)_x^{(0)}. \end{cases} \quad (44)$$

And in the schemes (31) – (32), the entries of the vector $P_x^x(t)$ are

$$\begin{aligned} \left(P_x^x(t)\right)_{i,j,k} = \frac{-2\pi}{\mu\varepsilon}\Big(& d_{i,0}^{[2]}\sin(2\pi(1 + y_j + z_k) - 2\sqrt{3}\pi t) \\ &+ d_{i,N_x}^{[2]}\sin(2\pi(-1 + y_j + z_k) - 2\sqrt{3}\pi t) \\ &+ d_{j,0}^{[2]}\sin(2\pi(x_i + 1 + z_k) - 2\sqrt{3}\pi t) \\ &+ d_{j,N_y}^{[2]}\sin(2\pi(x_i - 1 + z_k) - 2\sqrt{3}\pi t) \\ &+ d_{k,0}^{[2]}\sin(2\pi(x_i + y_j + 1) - 2\sqrt{3}\pi t) \\ &+ d_{k,N_z}^{[2]}\sin(2\pi(x_i + y_j - 1) - 2\sqrt{3}\pi t)\Big), \end{aligned}$$

for $i = 1, 2, \ldots, \overline{N}_x, j = 1, 2, \ldots, \overline{N}_y, k = 1, 2, \ldots, \overline{N}_z$. And

$$P_y^y(t) = -2P_x^x(t),\ P_z^z(t) = P_x^x(t),$$
$$Q_x^x(t) = \sqrt{3}P_x^x(t),\ Q_y^y(t) = \mathbf{0},\ Q_z^z(t) = -\sqrt{3}P_x^x(t).$$

From the schemes (31) – (32), we can obtain the numerical electric divergence $\left(E^x\right)_x^{(n)} + \left(E^y\right)_y^{(n)} + \left(E^z\right)_z^{(n)}$ and the numerical magnetic divergence $\left(H^x\right)_x^{(n)} + \left(H^y\right)_y^{(n)} + \left(H^z\right)_z^{(n)}$.

As the first problem, we investigate it in detail. And again in the second example, we present the description of the initial values and the vectors in numerical integration formula in the schemes (29) – (30) and the schemes (31) – (32).

Problem 2: We consider the the solutions

$$\begin{aligned} \mathcal{E}_x &= \frac{k_y - k_z}{\varepsilon\sqrt{\mu\omega}}\cos(\omega\pi t)\cos(k_x\pi x)\sin(k_y\pi y)\sin(k_z\pi z), \\ \mathcal{E}_y &= \frac{k_z - k_x}{\varepsilon\sqrt{\mu\omega}}\cos(\omega\pi t)\sin(k_x\pi x)\cos(k_y\pi y)\sin(k_z\pi z), \\ \mathcal{E}_z &= \frac{k_x - k_y}{\varepsilon\sqrt{\mu\omega}}\cos(\omega\pi t)\sin(k_x\pi x)\sin(k_y\pi y)\cos(k_z\pi z), \end{aligned} \quad (45)$$

and

$$\begin{aligned} \mathcal{H}_x &= \sin(\omega\pi t)\sin(k_x\pi x)\cos(k_y\pi y)\cos(k_z\pi z), \\ \mathcal{H}_y &= \sin(\omega\pi t)\cos(k_x\pi x)\sin(k_y\pi y)\cos(k_z\pi z), \\ \mathcal{H}_z &= \sin(\omega\pi t)\cos(k_x\pi x)\cos(k_y\pi y)\sin(k_z\pi z), \end{aligned} \quad (46)$$

where $\omega^2 = (k_x^2 + k_y^2 + k_z^2)/(\varepsilon\mu)$, $k_x = 1$, $k_y = 2$, $k_z = -3$, $\varepsilon = 1$, and $\mu = 1$. We consider the Dirichlet boundary conditions and take the analytical solutions (45) and (46) at $t = 0$ as the initial conditions, on a cube $\Omega = [-1, 1]^3$. Namely we have the numerical electric field vectors at initial time $E_x^{(0)}$, $E_y^{(0)}$, and $E_z^{(0)}$ with the entries

$$\begin{cases} \left(E_x\right)_{i,j,k}^{(0)} = \frac{k_y - k_z}{\varepsilon\sqrt{\mu\omega}}\cos(k_x\pi x_i)\sin(k_y\pi y_j)\sin(k_z\pi z_k), \\ \left(E_y\right)_{i,j,k}^{(0)} = \frac{k_z - k_x}{\varepsilon\sqrt{\mu\omega}}\sin(k_x\pi x_i)\cos(k_y\pi y_j)\sin(k_z\pi z_k), \\ \left(E_z\right)_{i,j,k}^{(0)} = \frac{k_x - k_y}{\varepsilon\sqrt{\mu\omega}}\sin(k_x\pi x_i)\sin(k_y\pi y_j)\cos(k_z\pi z_k), \end{cases} \quad (47)$$

for $i = 1, 2, \ldots, \overline{N}_x, j = 1, 2, \ldots, \overline{N}_y, k = 1, 2, \ldots, \overline{N}_z$, and the corresponding numerical curls of magnetic field vectors, $\widetilde{H}_x^{(0)}$, $\widetilde{H}_y^{(0)}$, and $\widetilde{H}_z^{(0)}$ as follows:

$$\widetilde{H}_x^{(0)} = \widetilde{H}_y^{(0)} = \widetilde{H}_z^{(0)} = \mathbf{0}. \quad (48)$$

The numerical magnetic field vectors at initial time $H_x^{(0)}$, $H_y^{(0)}$, and $H_z^{(0)}$ are expressed as follows:

$$H_x^{(0)} = H_y^{(0)} = H_z^{(0)} = \mathbf{0}. \quad (49)$$

And the corresponding numerical curls of electric field vectors, $\widetilde{E}_x^{(0)}$, $\widetilde{E}_y^{(0)}$, and $\widetilde{E}_z^{(0)}$ have the entries with the

following expression:

$$\begin{cases} \left(\widetilde{E}_x\right)^{(0)}_{i,j,k} = -\mu\omega\pi \sin(k_x\pi x_i)\cos(k_y\pi y_j)\cos(k_z\pi z_k), \\ \left(\widetilde{E}_y\right)^{(0)}_{i,j,k} = -\mu\omega\pi \cos(k_x\pi x_i)\sin(k_y\pi y_j)\cos(k_z\pi z_k), \\ \left(\widetilde{E}_z\right)^{(0)}_{i,j,k} = -\mu\omega\pi \cos(k_x\pi x_i)\cos(k_y\pi y_j)\sin(k_z\pi z_k), \end{cases} \tag{50}$$

for $i = 1, 2, \ldots, \overline{N}_x, j = 1, 2, \ldots, \overline{N}_y, k = 1, 2, \ldots, \overline{N}_z$.

In the schemes (29) – (30), the entries of the vector $P_x(t)$ are

$$\begin{aligned} \left(P_x(t)\right)_{i,j,k} = \frac{1}{\mu\varepsilon}\frac{k_y - k_z}{\varepsilon\sqrt{\mu}\omega}\cos(\omega\pi t)\Big(& \\ & d^{[2]}_{i,0}\cos(k_x\pi)\sin(k_y\pi y_j)\sin(k_z\pi z_k) \\ & +d^{[2]}_{i,N_x}\cos(-k_x\pi)\sin(k_y\pi y_j)\sin(k_z\pi z_k) \\ & +d^{[2]}_{j,0}\cos(k_x\pi x_i)\sin(k_y\pi)\sin(k_z\pi z_k) \\ & +d^{[2]}_{j,N_y}\cos(k_x\pi x_i)\sin(-k_y\pi)\sin(k_z\pi z_k) \\ & +d^{[2]}_{k,0}\cos(k_x\pi x_i)\sin(k_y\pi y_j)\sin(k_z\pi) \\ & +d^{[2]}_{k,N_z}\cos(k_x\pi x_i)\sin(k_y\pi y_j)\sin(-k_z\pi)\Big), \end{aligned}$$

and the other five vectors $P_y(t)$, $P_z(t)$, $Q_x(t)$, $Q_y(t)$ and $Q_z(t)$ can be obtained similarly. The initial values of the numerical discrete divergencies can be calculated exactly from the initial conditions (47), (48), (49), and (50). Precisely the vectors $\left(E^x\right)^{(0)}_x$, $\left(E^y\right)^{(0)}_y$, and $\left(E^z\right)^{(0)}_z$ are given as follows:

$$\begin{cases} \left(E^x\right)^{(0)}_x = -k_x(k_y - k_z)W_1, \\ \left(E^y\right)^{(0)}_y = -k_y(k_z - k_x)W_1, \\ \left(E^z\right)^{(0)}_z = -k_z(k_x - k_y)W_1, \end{cases} \tag{51}$$

where the entries of W_1 can be given as

$$\left(W_1\right)_{i,j,k} = \frac{\pi}{\varepsilon\sqrt{\mu}\omega}\sin(k_x\pi x_i)\sin(k_y\pi y_j)\sin(k_z\pi z_k),$$

for $i = 1, 2, \ldots, \overline{N}_x, j = 1, 2, \ldots, \overline{N}_y, k = 1, 2, \ldots, \overline{N}_z$. And the corresponding numerical curls of magnetic field vectors, $\left(\widetilde{H}^x\right)^{(0)}_x$, $\left(\widetilde{H}^y\right)^{(0)}_y$, and $\left(\widetilde{H}^z\right)^{(0)}_z$ are

$$\left(\widetilde{H}^x\right)^{(0)}_x = \left(\widetilde{H}^y\right)^{(0)}_y = \left(\widetilde{H}^z\right)^{(0)}_z = \mathbf{0}. \tag{52}$$

The numerical magnetic field vectors $\left(H^x\right)^{(0)}_x$, $\left(H^y\right)^{(0)}_y$, and $\left(H^z\right)^{(0)}_z$ are expressed as follows:

$$\left(H^x\right)^{(0)}_x = \left(H^y\right)^{(0)}_y = \left(H^z\right)^{(0)}_z = \mathbf{0}. \tag{53}$$

And the corresponding numerical curls of electric field vectors, $\left(\widetilde{E}^x\right)^{(0)}_x$, $\left(\widetilde{E}^y\right)^{(0)}_y$, and $\left(\widetilde{E}^z\right)^{(0)}_z$ have the following expression:

$$\begin{cases} \left(\widetilde{E}^x\right)^{(0)}_x = k_x W_2, \\ \left(\widetilde{E}^y\right)^{(0)}_y = k_y W_2, \\ \left(\widetilde{E}^z\right)^{(0)}_z = k_z W_2, \end{cases} \tag{54}$$

where the entries of W_2 are given as

$$\left(W_2\right)_{i,j,k} = -\mu\omega\pi^2\cos(k_x\pi x_i)\cos(k_y\pi y_j)\cos(k_z\pi z_k),$$

for $i = 1, 2, \ldots, \overline{N}_x, j = 1, 2, \ldots, \overline{N}_y, k = 1, 2, \ldots, \overline{N}_z$.

In the schemes (31) – (32), the entries of the vector $P^x_x(t)$ are

$$\begin{aligned} \left(P^x_x(t)\right)_{i,j,k} = \frac{1}{\mu\varepsilon}\frac{k_y - k_z}{\varepsilon\sqrt{\mu}\omega}(-k_x\pi)\cos(\omega\pi t)\Big(& \\ & d^{[2]}_{i,0}\sin(k_x\pi)\sin(k_y\pi y_j)\sin(k_z\pi z_k) \\ & +d^{[2]}_{i,N_x}\sin(-k_x\pi)\sin(k_y\pi y_j)\sin(k_z\pi z_k) \\ & +d^{[2]}_{j,0}\sin(k_x\pi x_i)\sin(k_y\pi)\sin(k_z\pi z_k) \\ & +d^{[2]}_{j,N_y}\sin(k_x\pi x_i)\sin(-k_y\pi)\sin(k_z\pi z_k) \\ & +d^{[2]}_{k,0}\sin(k_x\pi x_i)\sin(k_y\pi y_j)\sin(k_z\pi) \\ & +d^{[2]}_{k,N_z}\sin(k_x\pi x_i)\sin(k_y\pi y_j)\sin(-k_z\pi)\Big). \end{aligned}$$

Here we omit the detail about $P^y_y(t)$, $P^z_z(t)$, $Q^x_x(t)$, $Q^y_y(t)$ and $Q^z_z(t)$.

In the numerical simulations, we set $p = 3$, $N_x = N_y = N_z = N = 18$, the nodes c_i and coefficients b_i, for $i = 1, 2, 3$, of numerical integration formula are chosen (see paper [33]) as $c_1 = \frac{5-\sqrt{15}}{10}$, $c_2 = \frac{1}{2}$, $c_3 = \frac{5+\sqrt{15}}{10}$, $b_1 = \frac{5}{18}$, $b_2 = \frac{4}{9}$ and $b_3 = \frac{5}{18}$.

A. ERROR ESTIMATES AND NUMERICAL DISCRETE DIVERGENCIES

In this subsection, we simulate and present the maximum errors of method by solving Problem 1 and Problem 2, on the time interval [0, 12]. We show the approximate errors of the method with respect to different time stepsizes h_t, and the result is indicated in Figs. 1 and 2. It can be observed that the accuracy of the methods is sensitive and dependent on the time stepsize h_t.

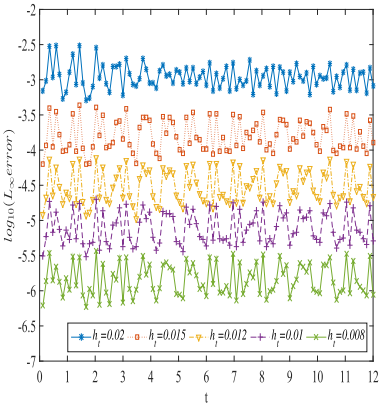

FIGURE 1. The maximum errors in numerical fields for problem 1.

Now we consider the time-approximation order of the method which can be obtained by using the following formula

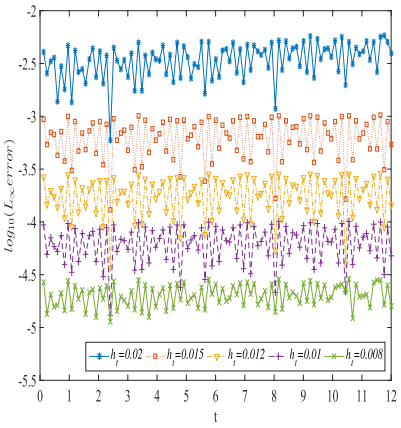

FIGURE 2. The maximum errors in numerical fields for problem 2.

TABLE 1. The maximum error at $T = 12$ and the numerical order of our schemes to solve problem 1.

	error	order
$h_t = 0.02$	$8.1264e-04$	$--$
$h_t = 0.015$	$1.2867e-04$	6.4066
$h_t = 0.012$	$2.1958e-05$	7.9235
$h_t = 0.01$	$5.0972e-06$	8.0102
$h_t = 0.008$	$8.7498e-07$	7.8974

TABLE 2. The maximum error at $T = 12$ and the numerical order of our schemes to solve problem 2.

	error	order
$h_t = 0.02$	$3.9567e-03$	$--$
$h_t = 0.015$	$5.3808e-04$	6.9352
$h_t = 0.012$	$1.4442e-04$	5.8943
$h_t = 0.01$	$4.7679e-05$	6.0786
$h_t = 0.008$	$1.5962e-05$	4.9038

(see, e.g. [3])

$$Order = \frac{\log Error_{\tau_2} - \log Error_{\tau_1}}{\log \tau_2 - \log \tau_1}, \tag{55}$$

where $\tau_i = h_{ti}$ for $i = 1, 2$. It can be observed from Tables. 1 and 2 that the method is of high order.

The main advantage of our method is the property of divergence-free. In this subsection, we will examine it numerically.

We show the quantity $E_x^x + E_y^y + E_z^z + (6-i) \times 10^{-16}$ in Fig. 3, and the quantity $H_x^x + H_y^y + H_z^z + (6-i) \times 10^{-16}$ in Fig. 4, for the method with the i-th time stepsize, where the vector of time stepsize is $h_t = (0.02,\ 0.015,\ 0.012,\ 0.01,\ 0.008)^\top$, for Problem 1. The last term $(6-i) \times 10^{-16}$ is added to the corresponding numerical divergence, for distinguishing the five curves, otherwise these curves will be overlapped completely. It can be seen from Figs. 3 and 4 that these numerical divergences are all zeros exactly.

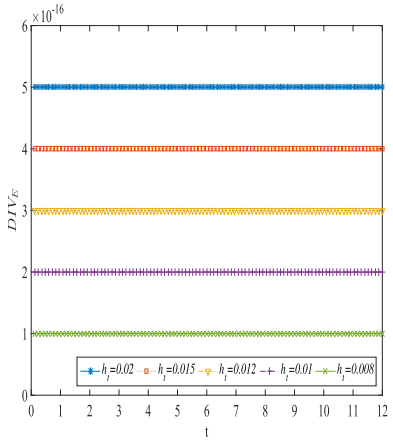

FIGURE 3. The numerical electric divergences for problem 1.

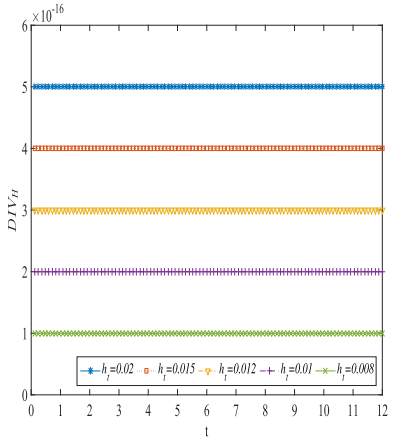

FIGURE 4. The numerical magnetic divergences for problem 1.

To verify the exact divergence-free, we draw the sum of E_y and $2E_x$, the difference between E_z and E_x, the sum of H_z and H_x, and H_y in Fig. 5; and the sum of E_y^y and $2E_x^x$, the difference between E_z^z and E_x^x, the sum of H_z^z and H_x^x, and H_y^y in Fig. 6; where the time stepsize is $h_t = 0.015$. It can be seen from the Figs. 5 and 6 that our scheme can preserve the proportional among the different fields of analytical solutions in numerical simulations.

For Problem 2, Figs. 7 and 8 presents the accuracy of the numerical divergences. We can see that our method is divergence-free and the accuracy is about $\mathcal{O}(10^{-13})$. Moreover, the larger time stepsizes can be used.

B. COMPUTATIONAL EFFICIENCY

In this subsection, we show the logarithm of the maximum global errors of fields against the CPU time at the final time $T = 12$. We use two AVF methods shown in [38] and [37] (denoted as AVF1 and AVF2 in [38]) for comparison.

In fixed-point iteration, we set the error tolerance as 10^{-15} and set the maximum number of iteration as 10. We choose

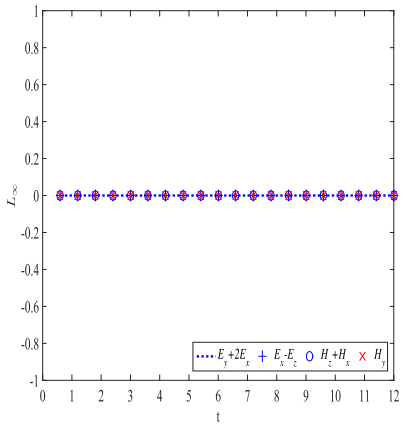

FIGURE 5. The linearity of problem 1.

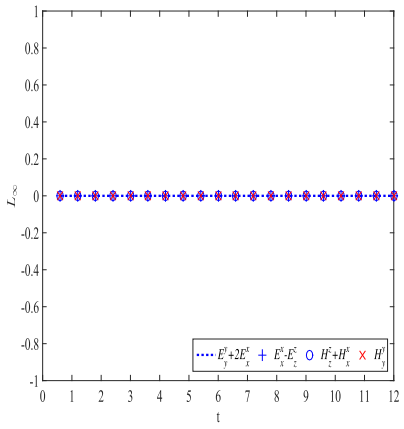

FIGURE 6. The linearity related to the numerical divergence for problem 1.

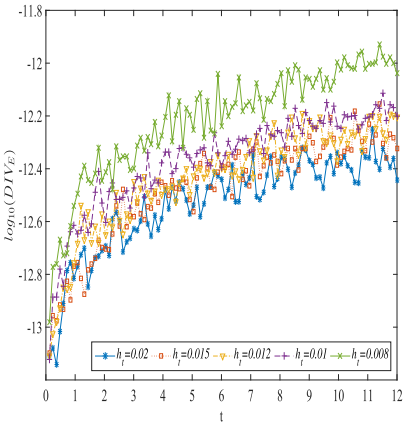

FIGURE 7. The numerical electric divergences for problem 2.

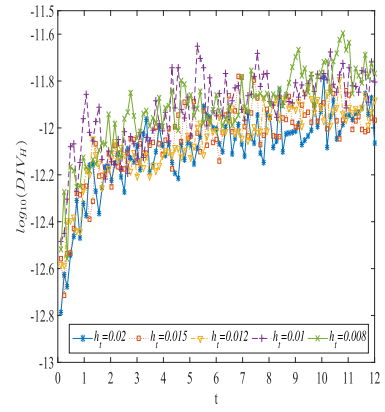

FIGURE 8. The numerical magnetic divergences for problem 2.

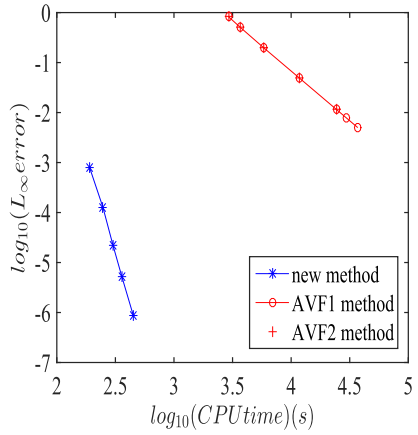

FIGURE 9. The numerical efficiency for problem 1.

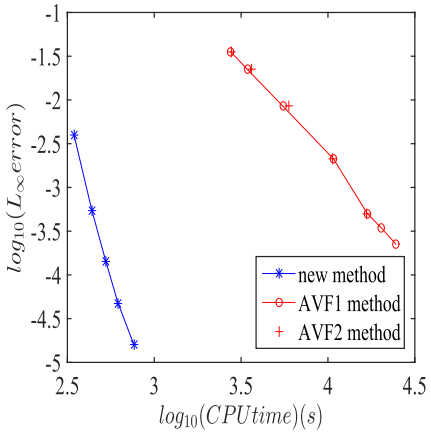

FIGURE 10. The numerical efficiency for problem 1.

the values of numerical solution at the previous step as the starting values for the iteration, at each time-cycle. The results are shown in Figs. 9 and 10, for Problem 1 and 2, respectively.

The numerical experiments show that the class of methods in this paper can be implemented with low computational cost.

V. CONCLUSION

Time-domain electromagnetics plays an important role in many numerical sciences, for example communications, computer networks, electronic engineering, radar, ground features detection, electromagnetic compatibility and biological electromagnetics.

Although in the numerical computation of Maxwell's equations, the methods in frequency-domain are successful and popular, the disastrous computational costs is the inherent deficiency of the frequency-domain methods, since sufficient sampling data is needed in the discrete Fourier transform to obtain the required solution. In our opinion, the small costs is exactly the charming of the direct time-domain method to us which is superior to frequency-domain method, since the number of collocation points can be very small. In a word, the direct time-domain methods is the most direct and natural means to compute time-domain Maxwell's equations.

Comparing to the traditional time-domain methods, for example, the integral equation method, the finite element method, and the finite difference method, this class of methods in this paper is the semi-discrete method which is normally explicit, robust and easy to code. As an example, we have the class of methods in [44] which is presented specially for Maxwell's equations with periodic boundary conditions in the rectangular coordinates. And in this paper, we discuss a class of explicit semi-discrete methods for Maxwell's equations with Dirichlet boundary conditions in similar way.

This paper focuses on the numerical solutions of Maxwell's equations in the rectangular coordinate system under the initial conditions and the Dirichlet boundary conditions, on source-free fields. The class of methods is simple and robust which bases on formulae (23) – (26), using the operator spectrum theory for electromagnetics. In the formulation of our methods, the key is the introduction of two matrix functions $\phi_0\left(h_t^2 L\right)$ and $\phi_1\left(h_t^2 L\right)$, where the differentiation matrix L of the operator $-\frac{1}{\mu\varepsilon}\nabla^2$ is positive definite. The numerical results show that our methods are explicit. Actually, we remark that the amazing of our methods lies in its explicit formation in the numerical computation, since it can overcome high computational complexity and expensive computational cost which occurs in the traditional numerical computation of the time-domain Maxwell's equations in three dimensions (since normally most of the methods in the literature are implicit).

At last, we point out that the other remarkable feature of our methods is the divergence-free. As known the divergence-free of electromagnetic fields is of importance in practicing scientists and engineers.

ACKNOWLEDGMENT

The authors would like to express sincere gratitude to the referees for their insightful comments and suggestions.

REFERENCES

[1] F. Assous, P. Degond, E. Heintze, P. A. Raviart, and J. Segre, "On a finite-element method for solving the three-dimensional Maxwell equations," *J. Comput. Phys.*, vol. 109, no. 2, pp. 222–237, Dec. 1993.

[2] C. A. Balanis, *Advanced Engineering Electromagnetics*. Hoboken, NJ, USA: Wiley, 2012.

[3] J. Cai, Y. Wang, and Y. Gong, "Numerical analysis of AVF methods for three-dimensional time-domain Maxwell's equations," *J. Sci. Comput.*, vol. 66, no. 1, pp. 141–176, Jan. 2016.

[4] J. Cai, Y. Wang, and Y. Gong, "Convergence of time-splitting energy-conserved symplectic schemes for 3D Maxwell's equations," *Appl. Math. Comput.*, vol. 265, pp. 51–67, Aug. 2015.

[5] W. Chen, X. Li, and D. Liang, "Energy-conserved splitting finite-difference time-domain methods for Maxwell's equations in three dimensions," *SIAM J. Numer. Anal.*, vol. 48, no. 4, pp. 1530–1554, Jan. 2010.

[6] W. Chen, X. Li, and D. Liang, "Energy-conserved splitting FDTD methods for Maxwell's equations," *Numerische Mathematik*, vol. 108, pp. 445–485, Nov. 2008.

[7] A. D. Chave, "Numerical integration of related Hankel transforms by quadrature and continued fraction expansion," *Geophysics*, vol. 48, no. 12, pp. 1671–1686, Dec. 1983.

[8] A. Dedner, F. Kemm, D. Kröner, C.-D. Munz, T. Schnitzer, and M. Wesenberg, "Hyperbolic divergence cleaning for the MHD equations," *J. Comput. Phys.*, vol. 175, pp. 645–673, Jan. 2002.

[9] P. A. Eaton, "3D electromagnetic inversion using integral equation," *Geophys. Prospecting*, vol. 37, pp. 407–426, May 1989.

[10] C. R. Evans and J. F. Hawley, "Simulation of magnetohydrodynamic flows: A constrained transport method," *Astrophys. J.*, vol. 332, pp. 659–677, Sep. 1998.

[11] R. Holland, "Finite-difference solution of Maxwell's equations in generalized nonorthogonal coordinates," *IEEE Trans. Nucl. Sci.*, vol. NS-30, pp. 4589–4591, Dec. 1983.

[12] P. Janhunen, "A positive conservative method for magnetohydrodynamics based on HLL and roe methods," *J. Comput. Phys.*, vol. 160, no. 2, pp. 649–661, May 2000.

[13] B.-N. Jiang, *The Least-Squares Finite Element Method: Theory and Applications in Computational Fluid Dynamics and Electromagnetics*. Berlin, Germany: Springer, 1998, pp. 47–80.

[14] B.-N. Jiang, J. Wu, and L. A. Povinelli, "The origin of spurious solutions in computational electromagnetics," *J. Comput. Phys.*, vol. 125, no. 1, pp. 104–123, Apr. 1996.

[15] T. Kato, *Perturbation Theory for Linear Operators*. New York, NY, USA: Springer-Verlag, 1966, pp. 1–60.

[16] L. Kong, J. Hong, and J. Zhang, "Splitting multi-symplectic integrators for Maxwell's equations," *J. Comput. Phys.*, vol. 229, pp. 4259–4278, Jun. 2010.

[17] J. Lee and B. Fornberg, "A split step approach for the 3-D Maxwell's equations," *J. Comput. Appl. Math.*, vol. 158, no. 2, pp. 485–505, Sep. 2003.

[18] D. Liang and Q. Yuan, "The spatial fourth-order energy-conserved S-FDTD scheme for Maxwell's equations," *J. Comput. Phys.*, vol. 243, pp. 344–364, Jun. 2013.

[19] C. Liu and X. Wu, "Arbitrarily high-order time-stepping schemes based on the operator spectrum theory for high-dimensional nonlinear Klein–Gordon equations," *J. Comput. Phys.*, vol. 340, pp. 243–275, Jul. 2017.

[20] C. Liu and X. Wu, "An energy-preserving and symmetric scheme for nonlinear Hamiltonian wave equations," *J. Math. Anal. Appl.*, vol. 440, no. 1, pp. 167–182, Aug. 2016.

[21] C. Liu and X. Wu, "The boundness of the operator-valued functions for multidimensional nonlinear wave equations with applications," *Appl. Math. Lett.*, vol. 74, pp. 60–67, Dec. 2017.

[22] N. K. Madsen and R. W. Ziolkowski, "A three-dimensional modified finite volume technique for Maxwell's equations," *Electromagnetics*, vol. 10, nos. 1–2, pp. 147–161, Jan. 1990.

[23] L. Mei, L. Huang, X. Wu, and S. Huang, "Semi-analytical exponential RKN integrators for efficiently solving high-dimensional nonlinear wave equations based on FFT techniques," *Comput. Phys. Commun.*, vol. 243, pp. 68–80, Oct. 2019.

[24] J. C. Nedelec, "Mixed finite elements in R3," *Numer. Math.*, vol. 35, pp. 315–341, Sep. 1980.

[25] R. Peyret, *Spectral Methods for Incompressible Viscous Flow*. New York, NY, USA: Springer, 2001, pp. 50–62.

[26] R. Peyret and T. D. Taylor, *Computational Methods for Fluid Flow*. New York, NY, USA: Springer, 1983, pp. 41–80.

[27] K. G. Powell, "An approximate Riemann solver for magnetohydrodynamics," NASA Langley Res. Center, Hampton, VA, USA, Tech. Rep. ICASE-Report 94-24 (NASA CR-194902), Apr. 1994.

[28] G. R. W. Quispel and D. I. McLaren, "A new class of energy-preserving numerical integration methods," *J. Phys. A: Math. Theor.*, vol. 41, no. 4, Feb. 2008, Art. no. 045206.

[29] S. M. Rao, *Time Domain Electromagnetics*. New York, NY, USA: Academic, 1999, pp. 151–306.

[30] J. T. Smith, "Conservative modeling of 3-D electromagnetic fields, Part II: Biconjugate gradient solution and an accelerator," *Geophysics*, vol. 61, no. 5, pp. 1319–1324, Sep. 1996.
[31] A. Taflove, "Re-inventing electromagnetics: Supercomputing solution of Maxwell's equations via direct time integration on space grids," *Comput. Syst. Eng.*, vol. 3, nos. 1–4, pp. 153–168, Jan. 1992.
[32] P. E. Wannamaker, G. W. Hohmann, and W. A. SanFilipo, "Electromagnetic modeling of three dimensional bodies in layered earths using integral equations," *Geophysics*, vol. 49, pp. 60–74, Jan. 1984.
[33] B. Wang, H. Yang, and F. Meng, "Sixth-order symplectic and symmetric explicit ERKN schemes for solving multi-frequency oscillatory nonlinear Hamiltonian equations," *Calcolo*, vol. 53, pp. 1–14, Mar. 2016.
[34] X. Wu, L. Mei, and C. Liu, "An analytical expression of solutions to nonlinear wave equations in higher dimensions with Robin boundary conditions," *J. Math. Anal. Appl.*, vol. 426, no. 2, pp. 1164–1173, Jun. 2015.
[35] X. Wu, C. Liu, and L. Mei, "A new framework for solving partial differential equations using semi-analytical explicit RK(N)-type integrators," *J. Comput. Appl. Math.*, vol. 301, pp. 74–90, Aug. 2016.
[36] X. Wu and B. Wang, *Geometric Integrators for Differential Equations With Highly Oscillatory Solutions*. Beijing, China: Science Press, 2021, pp. 68–77.
[37] X. Wu, B. Wang, and W. Shi, "Efficient energy-preserving integrations for oscillatory Hamiltonian systems," *J. Comput. Phys.*, vol. 235, pp. 587–606, Feb. 2013.
[38] X. Wu, K. Liu, and W. Shi, *Structure-Preserving Algorithms for Oscillatory Differential Equations II*. Berlin, Germany: Springer, 2015, pp. 69–93.
[39] X. Wu, X. You, W. Shi, and B. Wang, "ERKN integrators for systems of oscillatory second-order differential equations," *Comput. Phys. Commun.*, vol. 181, no. 11, pp. 1873–1887, Nov. 2010.
[40] H. Yang and X. Wu, "Trigonometrically-fitted ARKN methods for perturbed oscillators," *Appl. Numer. Math.*, vol. 58, no. 9, pp. 1375–1395, Sep. 2008.
[41] H. Yang, X. Wu, X. You, and Y. Fang, "Extended RKN-type methods for numerical integration of perturbed oscillators," *Comput. Phys. Commun.*, vol. 180, no. 10, pp. 1777–1794, Oct. 2009.
[42] H. Yang, X. Zeng, X. Wu, and Z. Ru, "A simplified Nyström-tree theory for extended Runge–Kutta–Nyström integrators solving multi-frequency oscillatory systems," *Comput. Phys. Commun.*, vol. 185, pp. 2841–2850, Nov. 2014.
[43] H. Yang and X. Zeng, "A feasible and effective technique in constructing ERKN methods for multi-frequency multidimensional oscillators in scientific computation," *Numer. Algorithms*, vol. 76, no. 3, pp. 761–782, Nov. 2017.
[44] H. Yang, X. Zeng, and X. Wu, "A novel class of explicit divergence-free time-domain methods for efficiently solving Maxwell's equations," *Comput. Phys. Commun.*, vol. 268, Nov. 2021, Art. no. 108101.
[45] H. Yang, X. Zeng, and X. Wu, "An approach to solving Maxwell's equations in time-domain," *J. Math. Anal. Appl.*, vol. 518, Feb. 2023, Art. no. 126678.
[46] K. Yee, "Numerical solution of initial boundary value problems involving Maxwell's equations in isotropic media," *IEEE Trans. Antennas Propag.*, vol. AP-14, no. 3, pp. 302–307, May 1966.
[47] X. You, J. Zhao, H. Yang, Y. Fang, and X. Wu, "Order conditions for RKN methods solving general second-order oscillatory systems," *Numer. Algorithms*, vol. 66, no. 1, pp. 147–176, May 2014.
[48] X. Zeng, H. Yang, and X. Wu, "An improved tri-coloured rooted-tree theory and order conditions for ERKN methods for general multi-frequency oscillatory systems," *Numer. Algorithms*, vol. 75, no. 4, pp. 909–935, Aug. 2017.

XIANYANG ZENG received the B.S. degree in physics from Xiangfan University, Hubei, China, in 2003, the M.S. degree in optics from Zhejiang Normal University, Zhejiang, China, in 2009, and the Ph.D. degree in computational electromagnetics from Nanjing University, Nanjing, China, in 2018.

From 2009 to 2018, he was an Instructor at the Nanjing Institute of Technology, Nanjing. Since 2018, he has been a Vice Professor with the Nanjing Institute of Technology. He has authored four SCI papers, six Chinese core papers, and more than ten patents. His research interests include control theory and control engineering, aircraft control, electronic technology application, and computational electromagnetics.

Dr. Zeng received the several awards and honors, including the Nanjing Excellent Thesis Awards, in 2015 and 2018.

HONGLI YANG received the B.S. degree in information and computing sciences from Shanxi University, Shanxi, China, in 2003, the M.S. and Ph.D. degrees in mathematics from Nanjing University, Nanjing, China, in 2009.

In 2008, she visited with Tuebingen Unversity, Tuebingen, Germany, as a Joint Training Doctor. From 2010 to 2019, she was an Instructor with the Nanjing Institute of Technology, Nanjing. From 2016 to 2018, she was Postdoctoral Fellow of atmospheric science at Nanjing University. Since 2019, she has been a Vice Professor with the Nanjing Institute of Technology. She has authored eight SCI papers. Her research interests include the structure-preserving algorithms for differential equations, rooted-tree theory of ERKN methods, and computational electromagnetics.

Dr. Yang received the several awards and honors, including the Nanjing Excellent Thesis Awards, in 2015 and 2018.